Measuring various types of low-frequency noise in DC/DC switching converters

Varun John
Validation Engineer
Texas Instruments

Power-supply noise levels are critical in applications like phase-locked loops (PLLs), voltage-controlled oscillators (VCOs), analog-to-digital converters (ADCs) and amplifiers.

In telecommunication networks, the upconversion of low-frequency noise injected from the power supplies of local oscillators and amplifiers to the intermediate frequency (IF) level during mixing with the radio frequency (RF) signal results in sideband formation on both sides of the IF, leading to higher phase noise. Phase noise adds to root-mean-square (RMS) phase error during the detection of digitally modulated signals, thereby limiting the performance of the network [1]. This white paper explains sources of low-frequency noise in bipolar junction transistors (BJTs), metal-oxide semiconductor field-effect transistors (MOSFETs) and resistors, and how this noise propagates to the output voltage of a DC/DC converter. I'll also show you a setup for measuring the low-frequency noise spectrum of the output voltage of a DC/DC converter and use that setup to compare a low-frequency noise-optimized DC/DC converter's noise spectrum with a standard DC/DC converter.

Types of low-frequency noise

The different types of noise in integrated circuits (ICs) include flicker noise, thermal noise, shot noise, popcorn noise and generation-recombination noise. Flicker noise and thermal noise dominate the low-frequency output voltage noise spectrum of a DC/DC converter.

Flicker noise

Flicker noise, also known as 1/f noise, has been observed in all electronic devices under biasing, for frequencies from 10^{-6}Hz to a few hundreds of hertz.

Flicker noise originates as a result of the modulation of the conductance of a channel. **Equation 1** expresses the conductance (σ) of a semiconductor as a product of the carrier concentration and mobility:

$$\sigma = q(n\mu_e + p\mu_h)$$ (1)

where q is the charge of an electron; n and p are the concentrations of electrons and holes, respectively; and μ_e and μ_h are the electron and hole mobility in the material, respectively.

Two models in literature try to explain σ modulation: A number fluctuation model developed by McWhorter in 1957 [2] and a mobility fluctuation model developed by Hooge in 1969 [3].

The McWhorter model states that flicker noise is a surface phenomenon that originates from the variation of carrier concentrations caused by charge trapping in surface states. **Figure 1** shows the energy-band diagram of an N-channel metal-oxide semiconductor (NMOS) in inversion.
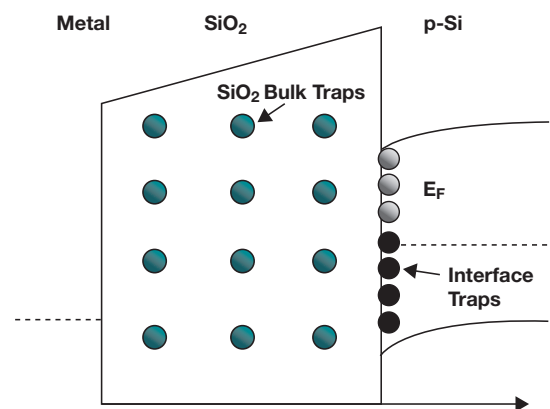

Figure 1. *Energy band diagram of an NMOS in inversion.*

Due to the imperfect interface between the silicon (Si) and silicon dioxide (SiO_2), there exist traps or intermediate energy states in the bandgap of the Si-SiO_2 interface. Defects in SiO_2 also lead to bulk SiO_2 traps. When applied to MOSFETs, the McWhorter theory states that the traps cause the trapping and release of carriers from the channel, thus causing a shift in the threshold voltage (V_t) and a fluctuation in carrier concentration [4] [5] [6]. The time constants for these transitions depend on the trap's distance from the surface. Traps that are much farther away have a smaller probability of trapping carriers.

In Hooge's mobility fluctuation model, flicker noise in semiconductor devices arises mainly from two carrier-scattering mechanisms: scattering in the semiconductor lattice and scattering from impurities. This model is more suitable to explain flicker noise in BJTs, whereas the McWhorter model better explains flicker noise in MOSFETs.

Thermal noise

Random charge carrier motion caused by thermal excitation in a resistive medium results in voltage fluctuations known as thermal noise. Thermal noise, also known as Johnson noise, is broadband white noise. **Equation 2** gives the spectral density of thermal noise across a resistor of resistance (R):

$$\overline{V_{th}^2} = 4kTR \times \Delta f \tag{2}$$

where k is the Boltzman constant, T is the absolute temperature, Δf is the frequency bandwidth and $4kT$ is equal to 1.61×10^{-20} VC at room temperature.

Thermal noise is often modeled as a voltage source in series with the resistor. A 50Ω resistor at room temperature has an associated noise voltage source of about $1nV/\sqrt{Hz}$, but this value increases with resistance.

Shot noise

Shot noise is a fluctuation in current caused by the discrete structure of charges composing it. Current flowing across a potential barrier is not uniform, but comprises individual carriers arriving at random times. The noise spectral density of shot noise given by Equation 3 is independent of temperature but proportional to the current flowing through the junction:

$$\overline{l_{sh}^2} = 2qI\Delta f \tag{3}$$

where *I* is the junction current.

Shot noise is modeled as a current source connected in parallel to the small-signal junction resistance. It is generally a low-noise contributor due to the low current in the reference system of a DC/DC converter.

Other sources of low-frequency noise in semiconductors include popcorn noise, also known as burst noise, or random-telegraph-signal (RTS) and generation-recombination noise. The RMS values of these noise sources are lower when compared to flicker and thermal noises for well-established fabrication technologies.

BJT and MOSFET noise models

Figure 2 shows equivalent BJT and MOSFET device models with noise sources included. In BJTs, the base layer has a certain resistance (r_b) that adds thermal noise. This can be modeled as a voltage source $\overline{v_{thr_b}^2}$ in series with r_b.

The base current in a BJT is the result of carrier injection from emitter to base and the recombination of these carriers in the base. These two processes are independent random events and thus have shot noise associated with them. The base current also has flicker noise from scattering mechanisms in the base.

You can combine these two noise sources, represented by a current source $\overline{l_{shb}^2} + \overline{l_{1/fb}^2}$ in parallel with the base-emitter junction. The collector current is made up of carriers diffusing through the base-emitter junction and accelerated by the field across the collector-base junction. The diffusion current is a random process and is a source of shot noise in the collector current. This is modeled as a current source in parallel to the collector-emitter terminals.

For MOSFETs, in addition to flicker noise, the resistance between drain and source causes thermal noise generated in the channel. You can combine the thermal and flicker noise together as a current source $\overline{l_{thd}^2} + \overline{l_{1/fb}^2}$ in parallel to the drain-source terminals.
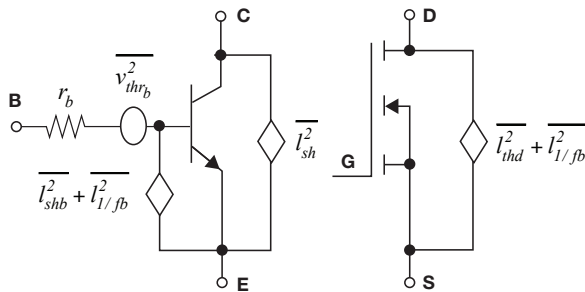
Figure 2. *Equivalent BJT and MOSFET noise models.*

Low-frequency output voltage noise in DC/DC converters

The low-frequency noise in the output voltage of DC/DC converters comes from the supply of the reference system and the internal transistors and resistors used in the reference system. This paper compares the low-frequency output noise spectral density of a DC/DC converter with a specially designed low-noise reference system (the

TPS63710) to a standard DC/DC buck converter (the TPS54622) that doesn't have any special noise-filtering schemes.

Since the TPS63710 is an inverting DC/DC converter that gives a negative output voltage for a positive input voltage, the TPS54622 is configured as an inverting buck-boost converter. Interchanging the V_{OUT} and GND pins configures a buck converter as an inverting buck-boost. Changing the FB resistor accordingly achieves the right output voltage. Reference [8] gives a detailed description on configuring a buck converter as a buck-boost.

Figure 3 shows the low-noise reference system of the TPS63710. External feedback resistors R_1 and R_2 and internal bandgap voltage (V_{BG}) set the value of the reference voltage (V_{REF}). The voltage at V_{REF} is negative and lower than the output voltage by the gain factor of the error amplifier. A resistor-capacitor (RC) filter made up of an internal 100K resistor and an external capacitor on the CAP pin filters the noise from the V_{REF} pin. The voltage on the CAP pin is the low-noise reference of the error amplifier. The output voltage Vout is reduced internally to $0.9*V_{OUT}$ before serving as the negative input of the error amplifier. The low gain (1/0.9) configuration of the error amplifier ensures that the noise from the error amplifier is not gained up.
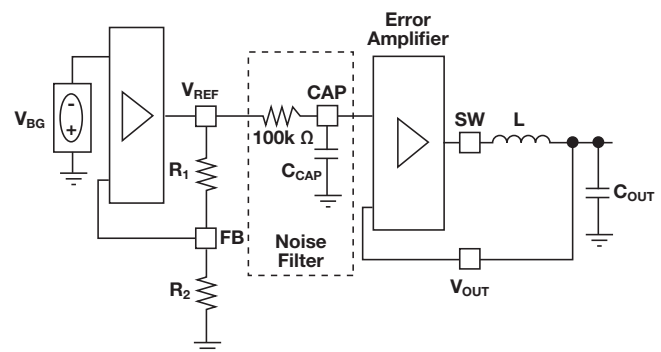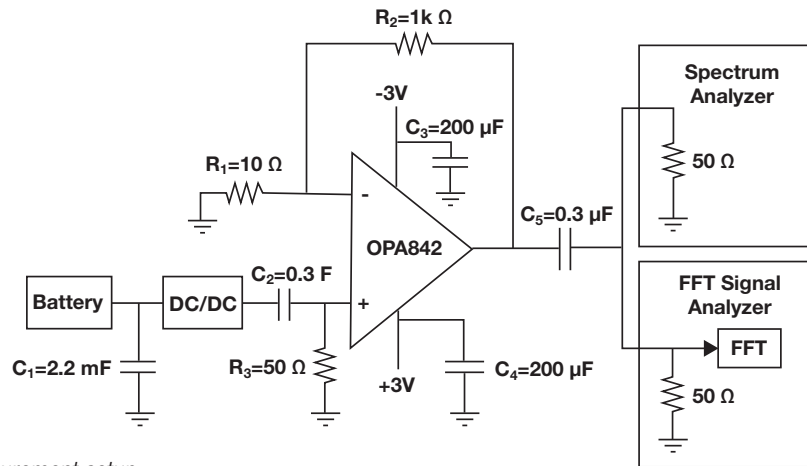

Figure 3. *TPS63710 low-noise reference system.*

Figure 4. *Noise measurement setup.*

Measurement setup for low-frequency noise

Figure 4 shows a setup for measuring the output voltage-noise spectrum of a DC/DC converter. You can measure the noise spectrum either with a heterodyne spectrum analyzer or a signal analyzer using the fast Fourier transform (FFT) function. I used a HP35670 FFT signal analyzer for the measurements shown in this paper because of the limitation of the spectrum analyzer to measure very low frequencies.

I recommend supplying the DC/DC converter and the operational amplifier (op amp) used in the setup with a battery at the input of the DC/DC converter to eliminate noise from the input power supply. Due to the limitations of the battery to supply high currents to the DC/DC converter, you could also use a low-noise bench power supply instead if the DC/DC converter under test has a high enough power-supply rejection ratio (PSRR) in the frequency band being measured. Most spectrum and signal analyzers only allow zero or very low DC voltage levels at their input. This necessitates the use of a DC blocker or high-pass filter at the DC/DC converter output.

Choose the capacitance C_2 so that the corner frequency of the C_2-R_3 high-pass filter is at least one

decade below the lowest measurable frequency. For example, a 0.3F capacitor with a 50Ω termination sets the corner frequency to 10mHz, with the lowest possible measurable frequency 100mHz.

Setting the OPA842 low-noise operational amplifier in a noninverting configuration with a gain of 100 amplifies the output voltage noise of the DC/DC converter over the noise floor of the signal analyzer. The HP35670 signal analyzer's noise floor was measured at around 300nV/$\sqrt{Hz}$.

It is important to not use large resistors at the inverting input of the op amp to avoid high thermal noise injection. Another high-pass filter at the output of the op amp made up of C_5 and the 50 Ω internal termination of the analyzers filters any DC offset at the op amp's output.

Figure 5 shows the noise spectral density of the output voltages of the TPS63710 and TPS54622. Both devices were supplied from a 6.5V battery source and V_{OUT} was set to −1.8V using the FB divider resistors. A 10µF capacitor on the CAP pin of the TPS63710 performed noise filtering. You can see that thermal noise dominates the noise spectrum of both devices from 1kHz upward. At lower frequencies, the influence of flicker noise starts increasing, dominating the total noise spectrum at very low frequencies.
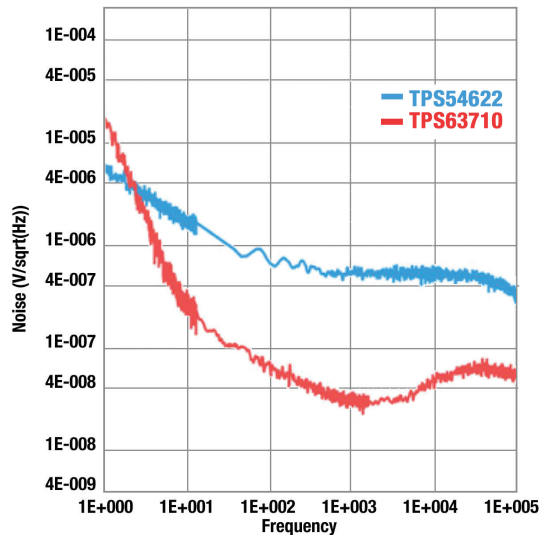
Figure 5. *Noise spectral density of the output voltage of TI's TPS54622 and TPS63710.*

Conclusion

Low-frequency noise from power supplies can limit the performance of noise-sensitive applications like telecommunications networks. Flicker and thermal noise dominates the noise in the output voltage spectrum of DC/DC converters. The low-noise reference system of the TPS63710, in combination with an external capacitor on the CAP pin, helps provide a negative output voltage with lower flicker and thermal noise levels.

References

1) Matt Loy. "Understanding and Enhancing Sensitivity in Receivers for Wireless Applications." Texas Instruments Technical Brief (SWRA30), May 1999.

2) Alan L. McWhorter. "1/f noise and germanium surface properties." Semiconductor Surface Physics, University of Pennsylvania Press (Philadelphia, Pennsylvania), 1957: 207-228.

3) F.N. Hooge. "1/f noise sources." IEEE Transactions on Electron Devices 41, No. 11 (November 1994): 1926-1935.

4) G. Reimbold. "Modified 1/f trapping noise theory and experiments in MOS transistors biased from weak to strong inversion – influence of interface states." IEEE Transactions on Electron Devices 31, No. 9 (September 1984): 1190-1198.

5) Kent H. Lundberg. "Noise Sources in Bulk CMOS," 2002.

6) Alicia Konczakowska and Bogdan M.Wilamowski. "Noise in Semiconductor Devices," 2010.

7) Yannis Tsividis. "Operation and Modeling of the MOS Transistor." McGraw-Hill (New York, New York), 1987.

8) Tahar Allag and Chris Glaser. "Using the TPS6215x in An Inverting Buck-Boost Topology." Texas Instruments Application Report (SL VA469C), November 2011 – Revised June 2013.